DALTON
FULL PAPER

X-Ray absorption spectroscopy studies on the structure of a biogenic "amorphous" calcium carbonate phase †

Yael Levi-Kalisman, Sefi Raz, Steve Weiner, Lia Addadi and Irit Sagi *

Department of Structural Biology, Weizmann Institute of Science, 76100 Rehovot, Israel. Fax: 972 - 8 - 9344136; E-mail: yael.levi@weizmann.ac.il; sefi.raz@weizmann.ac.il; steve.weiner@weizmann.ac.il; lia.addadi@weizmann.ac.il; irit.sagi@weizmann.ac.il

Received 25th April 2000, Accepted 8th June 2000
First published as an Advance Article on the web 20th September 2000

Amorphous calcium carbonate is formed by a surprisingly large number of organisms, bearing in mind how unstable it is. Organisms use amorphous calcium carbonate as temporary storage sites for ions, as precursor phases that transform into more stable crystalline calcium carbonate polymorphs, or in a stabilized form for mechanical purposes. Here one example is examined that fulfils the latter function; the so-called antler shaped spicules formed by the ascidian *Pyura pachydermatina*. These spicules are composed of amorphous calcium carbonate containing 16% (w/w) water and 14 mole% phosphate. A detailed X-ray absorption spectroscopy (XAS) study of the calcium K-edge in the spicules shows a first co-ordination shell with seven/eight oxygen atoms, and a second co-ordination shell with four/five carbon atoms. The best fit was obtained using monohydrocalcite as model, and is consistent with a slightly expanded hydrated structure. It is noteworthy that the XAS spectrum of these spicules is quite different from that reported previously for the amorphous calcium carbonate of plant cystoliths. This raises the intriguing possibility that the biogenic amorphous phases differ structurally from each other, and that the differences can account for their diverse modes of formation and function.

Introduction

The biomineralization world is rich in terms of the variety of minerals produced by organisms that differ in composition, structure, morphology, mechanical properties and functions. A survey of the known biogenic minerals shows that approximately 80% are crystalline and 20% are amorphous.[1] The proportion of the latter is probably underestimated due to the difficulty of detecting amorphous phases in the presence of crystalline materials. The amorphous metastable phase is either stabilized by the organism for its entire lifetime, or subsequently transforms into a more stable crystalline form. An important advantage of amorphous phases is their high solubility, allowing them to be deposited relatively easily and subsequently redissolved. This is consistent with their use in biology as a temporary storage site or as a transient phase prior to the deposition of a denser crystalline phase. Another advantage of using an amorphous phase is for mechanical support, as its isotropic properties facilitate equal distribution of mechanical stress. It is also easier to mold isotropic materials into complex shapes as compared to crystalline materials. For a review of amorphous minerals in biology see Simkiss.[2]

Silica (opal), which is a stable amorphous phase, is the most commonly formed biogenic amorphous mineral.[1] Other widely distributed biogenic amorphous minerals are amorphous calcium phosphates and amorphous calcium carbonates. Silica is formed by the polymerization of silicic acid[3] and its formation can be mediated enzymatically.[4,5] Silica is the mineral component of the skeletons of many microscopic sized organisms, such as diatoms and radiolarians. These often have exquisite morphological features characterized by smooth surfaces. In contrast to silica, which is a stable amorphous mineral, amorphous calcium carbonate and amorphous calcium phosphate tend to transform, in an uncontrolled environment, into a more stable crystalline phase. This transformation is both thermodynamically and kinetically favored under ambient conditions.[6] In biomineralization, however, both these phases may be stabilized, or if transformed this transformation is usually controlled by the organism leading to the formation of a particular crystalline phase.[1] In the teeth of the chiton *Acanthopleura*, for example, the initial deposit of the inner layer is amorphous calcium phosphate. After approximately two weeks it converts into dahllite.[7] Another example is the sea urchin embryo, which has an internal skeleton composed of two spicules, each of which is a single crystal of calcite.[8] Beniash *et al*.[9] showed that the formation of the spicule takes place by the transformation of amorphous calcium carbonate into calcite.

Amorphous calcium carbonate is significantly less stable than the other five forms of calcium carbonate: calcite, aragonite, vaterite, monohydrocalcite and calcium carbonate hexahydrate.[10] Nevertheless, certain organisms from different kingdoms and various phyla are known to form stable amorphous calcium carbonate. In particular, it is widespread in plants (kingdom *Plantae*) as cystoliths. Cystoliths are intracellular particles, made of amorphous calcium carbonate, that are found in great numbers in the leaves of higher plants.[11] The *Crustacea*[12] and a group within the *Chordata* called the *Ascidiaceae*[13,14] also produce amorphous calcium carbonate minerals. The ascidians (also known as the tunicates) form a diverse array of minerals. Many of the ascidians that form minerals are confined to one class, the *Pyuridae*. These deposit no less than six different minerals, including amorphous calcium phosphate and amorphous calcium carbonate.[15] *Pyura pachydermatina* (*Chordata*, *Ascidiacea*), the focus of this study, forms "dog bone"-shaped calcitic spicules in the tunic, and "antler-shaped" spicules in the body tissues. The antler-

† Based on the presentation given at Dalton Discussion No. 3, 9–11th September 2000, University of Bologna, Italy.

Electronic supplementary information (ESI) available: EXAFS spectra. See http://www.rsc.org/suppdata/dt/b0/b003242p/

shaped spicules are composed entirely of amorphous calcium carbonate,[16] which is stable throughout the lifetime of the organism. Little is known about the mechanism by which this stabilization is achieved. Aizenberg *et al*.[13] showed that both these antler spicules and spicules from the sponge *Clathrina*, which also contain stable amorphous calcium carbonate, have similar specialized macromolecules that can stabilize amorphous calcium carbonate *in vitro*. It was therefore suggested that these macromolecules are responsible for inhibition of crystallization, the consequent precipitation of an amorphous metastable phase, and its stabilization. Other studies showed that magnesium and phosphate may also participate in the stabilization of amorphous phases.[17–19] Indeed minor amounts of both magnesium and phosphorus are found in the antler spicules of *Pyura pachydermatina* and in many other amorphous calcium carbonate phases.[1,12,20]

The definition of an amorphous material is somewhat confusing. Not only is it technique dependent, but it is also characterized by the lack of certain properties rather than their presence. Amorphous materials are thus generally referred to as those that produce no X-ray and/or electron diffraction patterns. This implies that these materials have no long-range order. The local structure in amorphous calcium carbonate was studied by EXAFS for the first time by Taylor *et al*.[21] in cystoliths. It is likely that calcium carbonate materials that produce no diffraction pattern, but have different stoichiometries and different degrees of short-range order, have all been referred to as the same material, namely amorphous calcium carbonate. The possibility exists that the amorphous calcium carbonate phase of, for example, *Pyura pachydermatina* antler spicules may differ from other amorphous calcium carbonate phases, and that the differences may provide insight into the known variations in stabilities of these biogenic materials and their subsequent fate. This is the focus of this study.

Experimental

Materials

Single geological calcite crystals (Iceland Spar) from Mexico were purchased from Ward's (catalog number 49H1600). Geological aragonite was collected from the Dead Sea where it precipitated inorganically. Antler spicules from *Pyura pachydermatina* (Otago Harbour, Portobello, New Zealand) branchial sac tissue were isolated as described previously with ethanol, and preserved dry.[22]

EDS [energy dispersive (X-ray analysis) spectroscopy] analysis

The *Pyura* spicules were embedded in a mixture of Buehler ultramount powder and liquid, and polished using a MINIMET Buehler polisher to obtain a flat surface. The embedded sample was then placed on an aluminum stub coated with double-sided carbon tape. The conductivity was further increased using conductive carbon paste between the embedded sample and the aluminum stub, and the sample was carbon coated for SEM observation (JSM-6400) and EDS measurements (Oxford-ISIS). The phosphorus analysis was performed using SEMQuant with a standard of GaP for phosphorous analysis and wollastonite as a standard for calcium analysis.

TGA and DTA analyses

These were performed using a Shimadzu DTG-50 instrument equipped with microbalance. The *Pyura* antler spicules (3–5 mg) were placed in an aluminum pan and measured against a reference empty pan. The heating was performed in a nitrogen atmosphere (30 ml min^{-1}), with a heating rate of 10 °C min^{-1}. The baseline spectrum, obtained under the same conditions with two empty aluminum pans, was subtracted from the measurement spectrum.

X-Ray analysis

A powdered sample wetted by a few drops of absolute ethanol was pressed into a thin layer against a germanium holder surrounded with aluminum. The diffraction spectrum was collected using a Rigaku D/max-B diffractometer with Cu-Kα radiation at 50 kV and 150 mA. Each sample was scanned over a 2θ range of 5–60° with a scan speed of 0.3° min^{-1} and sampling interval of 0.02°.

Fourier transform infrared analysis

A powdered sample (approximately 0.1 mg) was mixed with about 10 mg of anhydrous KBr. The mixture was pressed into a 7 mm diameter pellet. The analysis was performed at 4 cm^{-1} resolution using a Midac Corporation FTIR spectrometer.

X-Ray absorption spectroscopy (XAS)

Sample preparation. Samples were ground in an agate mortar and filtered through a 400 mesh sieve. The powdered sample was loaded into a copper sample holder (10 × 5 × 0.5 mm) covered on both sides with polypropylene film. The latter was found to contain undetectable amounts of calcium.

Data collection. XAS data collection was performed at the National Synchrotron Light Source at Brookhaven National Laboratory, beam line X19A. The beam was run at an energy of 2.8 GeV with a beam current of approximately 200 mA. The spectra were recorded at the calcium K-edge in fluorescence geometry at room temperature under a helium atmosphere to minimize scattering. The incident beam intensity, I_0, was recorded using an ionization chamber. The fluorescence intensity was recorded using a PIPS detector. The transmission signal from a sample of geological calcite was measured simultaneously with fluorescence for the purpose of absolute energy calibration. Three scans were recorded for XANES spectra and nine scans for the EXAFS spectra. *Pyura* spicules checked by FTIR before and after exposure to X-rays showed no change in sample structure due to radiation damage.

Data processing and analysis. Smooth atomic background was removed with the AUTOBK program of the UWXAFS data analysis package, developed in the University of Washington, Seattle.[23] The *r*-space region for minimizing the signal below the first shell was chosen between 0 and 1 Å. The useful k range in the resultant k^2-weighted background subtracted spectra, $\chi(k)$, was between 2 and 10 $Å^{-1}$. Model data for the fitting procedure were constructed using the computer code ATOMS[24] based on the crystallographic data of each model compound: calcite,[25] aragonite,[25] $CaCO_3 \cdot H_2O$[26] and $CaCO_3 \cdot 6H_2O$.[18] Using the computer code FEFF7[27] we have calculated the theoretical photoelectron scattering amplitudes and phase shifts. The total theoretical $\chi(k)$ for each model was constructed by adding the most important $\chi(k)$'s paths that contributed to the r range of interest. The theoretical XAFS signal was fitted to the experimental data using the program FEFFIT[23] in r space, by Fourier transforming both theory and data. Curve-fitting analysis was conducted using standard procedures.[28]

Results

As reflected in their name, the antler spicules from *Pyura pachydermatina* have a very unique highly branched shape (Fig. 1). The branches are a few hundreds of microns in length and approximately 10 μm thick.[13] The *Pyura* antler spicules were first characterized using several different approaches, before performing a detailed study by X-ray absorption spectroscopy.

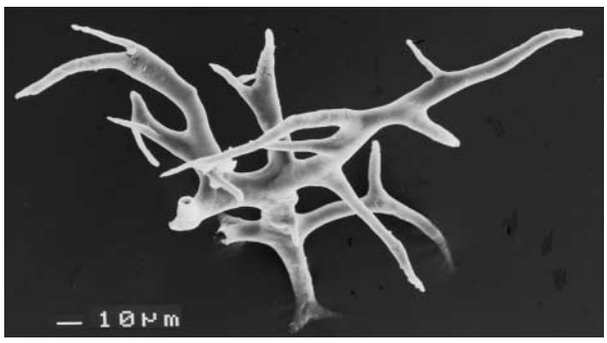

Fig. 1 Scanning electron micrograph of an antler spicule from *Pyura pachydermatina.*

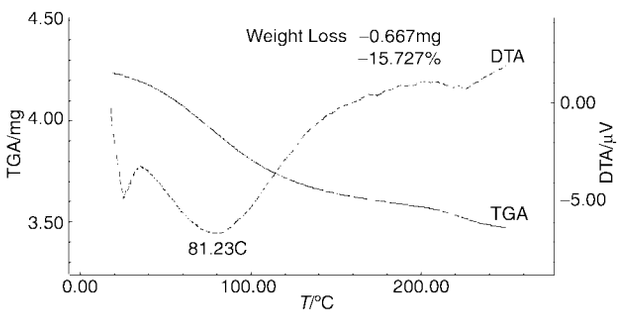

Fig. 2 Thermogravimetric analysis (TGA) and differential thermal analysis (DTA) of the antler spicules of *Pyura pachydermatina*. The weight loss of 15.727% relates to the temperature range 20–200 °C.

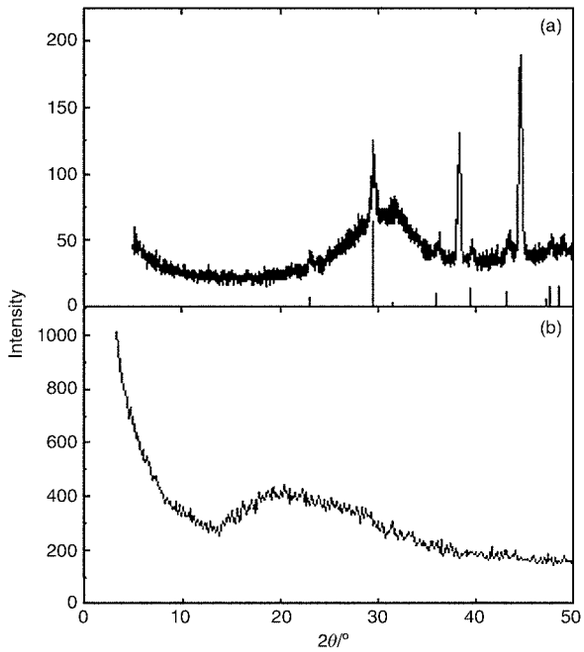

Fig. 3 X-Ray powder spectra. (a) *Pyura pachydermatina* antler spicules after thermal analyses. The thin lines represent the X-ray diffraction peaks of calcite for comparison. Al = aluminum peaks from the sample holder. (b) *Pyura pachydermatina* antler spicules. The spectrum was taken using synchrotron radiation.[13] The 2θ values were normalized to λ(Cu-Kα radiation) = 1.540598 Å.

Embedded and polished samples of the spicules were examined using Energy dispersive spectrometry. The spicules were found to contain 14(±2) mole% phosphate, homogeneously distributed throughout the spicule volume (within the spatial resolution of the measurement, ≈1 μm). Surprisingly, the infrared spectrum of these spicules does not show absorption peaks that can uniquely be attributed to a phosphate phase.[13] Examination of the antler spicules using TGA and DTA revealed that below 250 °C there are two distinguishable temperature intervals where weight losses occur. These are accompanied by broad endothermic peaks at 81 and 226 °C (Fig. 2). The most significant weight loss occurred in the temperature range of 20–200 °C and is attributed to the release of water molecules. The total weight loss in this transition is 15–16% (w/w). This result is compatible with a stoichiometry of one water molecule per carbonate ion for the amorphous phase, and is found to be in good agreement with the result obtained by Brecevic and Nielsen[10] for synthetic amorphous calcium carbonate. The second weight loss is 2–3% (w/w) and occurs in the temperature range of 200–250 °C. This loss is not likely to be caused by water release at such high temperatures, and is attributed to the release of CO_2 either of organic or inorganic origin. Fig. 3(a) shows the powder X-ray measurement of the antler spicules after thermal analyses. The spectrum is compatible with an amorphous phase, with a broad peak that is slightly shifted with respect to the one obtained from untreated antler spicules (Fig. 3b). In addition, the powder diffraction showed the existence of calcite in small amounts. The stabilization of the amorphous phase after exposure to a high temperature is probably due to the presence of phosphate ions. A FTIR measurement of the same sample (data not shown) confirmed that most of the material is indeed amorphous calcium carbonate.[9] The spectrum, however, shows a significant increase in the intensities of the phosphate peaks (relatively broad peak centered at 1062 cm^{-1} and a smaller peak at 583cm^{-1}) that does not reflect the approximate phosphate : carbonate ratio in the untreated sample. It is conceivable that these peaks increased due to some ordering of the phosphate ions caused by heating.

X-Ray absorption spectroscopy studies

XAS can be used to obtain structural information on the arrangement of atoms in the local environment of a central (absorbing) atom. Since long-range order is not required in this analysis, both crystalline and non-crystalline phases can be treated on the same basis. The near-edge structure (XANES) in an absorption spectrum covers the range between the threshold and the point where EXAFS (Extended X-Ray Absorption Fine Structure) begins. Qualitative spectral analysis in this region provides information about the chemical valency of the absorbing atom, and the symmetry of the surrounding near-neighbor atoms. The EXAFS region, above the absorption edge, can be interpreted in a highly quantitative way to determine co-ordination numbers, distances from neighboring atoms to the central atom, disorder parameters and types of atoms in the various co-ordination shells. We studied the local atomic environment around the calcium ion in amorphous calcium carbonate from the antler spicules of *Pyura pachydermatina*, using both XANES and EXAFS spectroscopy. FTIR spectra of the samples taken before and after exposure to X-rays showed no change in structure due to radiation damage.

Fig. 4 shows normalized absorption edge data of amorphous calcium carbonate from the antler spicules compared with the spectra of geological calcite and geological aragonite. Calcite and aragonite, having well characterized structures, serve as model compounds, as well as controls for our analysis methods. A significant difference in the XANES structure is observed between the amorphous calcium carbonate and the crystalline calcite and aragonite. There is a clear decrease in the number of features and their intensities in the edge spectra when moving from crystalline to amorphous material. This may indicate a reduction in order. In addition, a substantial change in the edge position is also detected, which implies a change in the partial oxidation state of the absorber and in the co-ordination numbers in the different samples.[29] The edge position shifts to higher energies from calcite, *via* amorphous calcium carbonate to aragonite. This result is consistent with our quantitative EXAFS analysis, which indeed shows an

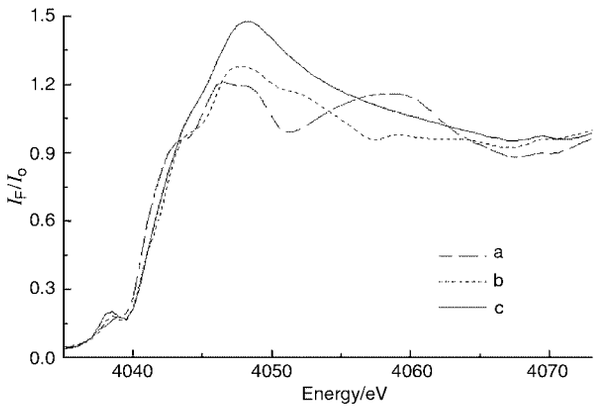

Fig. 4 Raw XANES region data of geological calcite (a), geological aragonite (b), and amorphous calcium carbonate from antler spicules of *Pyura pachydermatina* (c).

increase in co-ordination number from calcite, *via* the amorphous calcium carbonate to aragonite.

We have calibrated our curve-fitting procedure by analysing geological calcite and aragonite. Fitting the theoretical calcite model to the experimental data gave results which are in good agreement with the crystallographic data[30] (Table 1). The amorphous calcium carbonate was analysed using four different theoretical models, which were constructed from the crystal structures of calcite,[25] aragonite,[25] monohydrocalcite ($CaCO_3 \cdot H_2O$)[26] and calcium carbonate hexahydrate ($CaCO_3 \cdot 6H_2O$).[18] Calcite and aragonite are two crystalline polymorphs of calcium carbonate with different co-ordination numbers (6 and 9 respectively). Monohydrocalcite and calcium carbonate hexahydrate are crystalline polymorphs of calcium carbonate that contain water (in different amounts) in their structures. Although they have the same calcium–ligand arrangement in the first co-ordination shell (8 oxygen atoms), they have different numbers of carbon atoms in the second co-ordination shell due to the different amounts of water. Monohydrocalcite has three independent calcium ions per unit cell in its structure. They all have the same co-ordination number, but the oxygen atoms are located at slightly different distances from each of the calcium ions. Models of the theoretical EXAFS spectra were calculated by the computer code FEFF7[27] for each of the independent calcium ions separately.

The curve-fitting results of the amorphous calcium carbonate from the antler spicules are summarized in Table 2. Corrections to the energy origin (ΔE_0), bond distances (ΔR) and mean square disorders of the distances (Debye–Waller factors, $\Delta\sigma^2$) were varied until the best fit was obtained. In order to achieve the best theoretical model for fitting the experimental data various relevant structures were examined. The first shell was fitted using each of the three monohydrocalcite models (Ca1, Ca2, Ca3), in addition to the models of calcite, aragonite and calcium carbonate hexahydrate. The results obtained from this procedure show a good fit of the first shell in all models. Best fits, however, were obtained using calcite and monohydrocalcite (Ca3) as models. In the latter the fit was performed using each of the eight possible Ca–O paths separately and combined. The most stable fit was obtained using only one Ca–O path (O2). This implies a homogeneous distribution of the nearest neighbors (oxygen atoms) around the calcium ion.

Second shell analysis was performed using the following strategy. A fit to one Ca–C path was not satisfactory (*R* factor and χ^2 relatively high). Another Ca–C path was therefore added using the monohydrocalcite model, which improved the result (*R* factor = 0.000079; reduced χ^2 = 14.4). The *R* range for the fit was 1.2–3.3 Å. The shifts in origin energies for the first and second shell were found by stepping ΔE_0 for the first shell and varying ΔE_0 for the second shell until the best fit was achieved. Both ΔE_0's were then fixed to the values found (ΔE_0 (first shell) = 1.5, ΔE_0 (second shell) = 1.3 eV). The co-ordination numbers of the oxygen and carbon paths were floated, as were all the distances, and the following values were obtained. The Ca–O distance R_{Ca-O} was stable at 2.374 Å (±0.003), where 7.4 (±0.5) oxygen atoms were found to be located. The number of carbon atoms found at R_{Ca-C} = 3.03 Å (±0.03) was 1.5 (±0.7), and 3 (±1) carbon atoms were found at R_{Ca-C} = 3.36 Å (±0.01). In monohydrocalcite (Ca3) there are four carbon atoms at the following distances from the calcium: 2.7152, 2.8790, 3.1711 and 3.3189 Å. The results of the fit for the second shell thus show longer distances as compared to those of monohydrocalcite. This is expected for an amorphous material, as crystalline phases are known to be the most closely packed structures. The final results were obtained by fixing the Debye–Waller factor for the short carbon path at σ^2 = 0.006 Å^2 and varying the two other σ^2. The background-subtracted spectrum, $\chi(k)\cdot k^2$, and the fitted spectrum in *R* space, are shown in Fig. 5. The stability of the fitting result was examined by changing the initial conditions for the floated parameters and following the changes in *R* factor. It was further checked by constraining the co-ordination numbers to the values obtained and comparing the resultant distances and Debye–Waller factors (Table 2).

Following the results from EDS measurement, which showed the existence of about 14 mole% phosphate in the antler spicules, we examined the possibility of a substantial phosphate contribution to the EXAFS spectrum. A model where one Ca–P path was included in the structure was created by FEFF7. We used the ATOMS[24] code to calculate the co-ordination numbers and distances of the phosphorus atoms from calcium in hydroxyapatite.[31] Amongst these the Ca–O–P bond most similar to one of the (Ca3)–O–C bonds in monohydrocalcite was selected and inserted as the path of Ca–P contribution to the monohydrocalcite data file. FEFF7 was run to calculate the theoretical photoelectron scattering amplitudes and phase

Table 1 EXAFS curve-fitting results of experimental data from geological calcite to its calculated theoretical model compared with the crystallographic structure[30]

Atom type	Co-ordination no.	EXAFS		Crystallography
		R/Å	σ^2/Å^2	*R*/Å
O	6	2.367 ± 0.005	0.0066 ± 0.0009	2.360
C	6	3.21 ± 0.03	0.015 ± 0.005	3.21
O	6	3.52 ± 0.02	0.012 ± 0.003	3.46
Ca	6	4.11 ± 0.01	0.010 ± 0.002	4.05

Table 2 EXAFS curve-fitting results of amorphous calcium carbonate from the antler spicules of *Pyura pachydermatina*. The uncertainties are given for each varied parameter. The symbols f (fixed) and v (varied) indicate how the respective parameter was treated in the fit as described in text

	Fit to monohydrocalcite		
Atom type	Co-ordination no.	*R*/Å	σ^2/Å^2
O	7.4 ± 0.5 (v)	2.374 ± 0.003 (v)	0.009 ± 0.001 (v)
C	1.5 ± 0.7 (v)	3.03 ± 0.03 (v)	0.006 (f)
C	3 ± 1 (v)	3.36 ± 0.01 (v)	0.000 ± 0.004 (v)
	Fit with constrained co-ordination numbers		
O	7.4 (f)	2.374 ± 0.002 (v)	0.0089 ± 0.0003 (v)
C	1.5 (f)	3.03 ± 0.02 (v)	0.007 ± 0.004 (v)
C	3.0 (f)	3.364 ± 0.009 (v)	0.000 ± 0.001 (v)

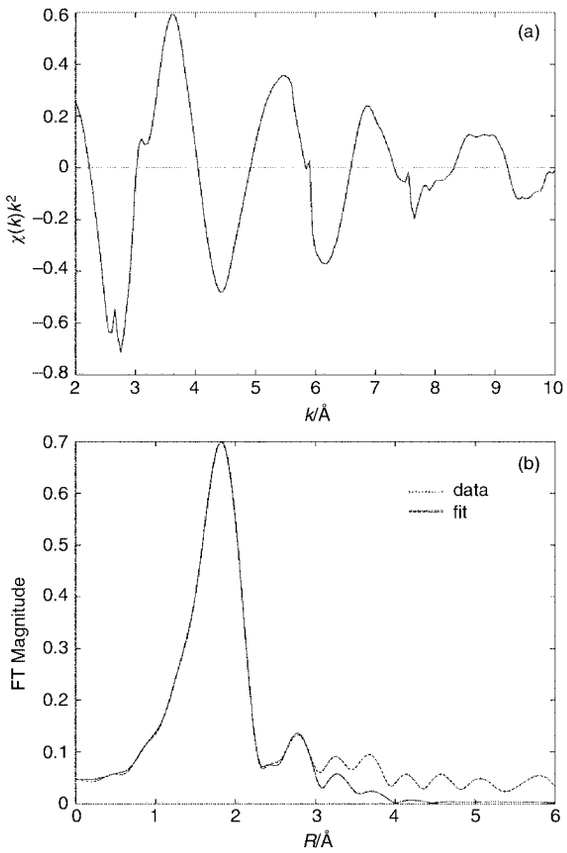

Fig. 5 (a) Background subtracted raw data of amorphous calcium carbonate from antler spicules of *Pyura pachydermatina* in k space. The useful k range in the resultant k^2-weighted $\chi(k)$ was between 2 and 10 $Å^{-1}$. Amplitudes and phase shifts of both theoretical and experimental data were weighted by k and multiplied by the Hanning window function in the Fourier transforms. (b) Representation of EXAFS fitting results in R space of experimental data (dotted line) and the calculated theoretical model from monohydrocalcite, Ca3 (solid line).

shifts to the new monohydrocalcite-like model structure. Other combinations of Ca–O–P bonds were also attempted. Under these conditions reasonable fit improvements could not be obtained, suggesting that the phosphate contribution to the spectrum, if at all present, is not substantial. Although the detection of a Ca–P contribution in the antler spicules could be, at the most, at the resolution limit of XAS, it was important to check that the effect of phosphate is not overwhelming.

Discussion

EDS, X-ray and TGA measurements were used to characterize biogenic amorphous calcium carbonate from the antler spicules of the ascidian *Pyura pachydermatina*. The spicule material is "amorphous" in that it produces no X-ray [13] diffraction pattern, and its infrared spectrum has broad peaks in the lattice frequency region. These are all characteristics of materials lacking long range order.

The calcium K-edge EXAFS data provide detailed information on the short-range structure of the spicule amorphous calcium carbonate. Six theoretical models (calcite, aragonite, monohydrocalcite: Ca1, Ca2 and Ca3 and calcium carbonate hexahydrate) were independently fitted to the EXAFS experimental data; of these monohydrocalcite (Ca3) led to the best fit. This is consistent with the TGA analysis, which indicated that the amorphous calcium carbonate has one water molecule per carbonate ion. According to the fit, 7.4 (±0.5) oxygen atoms are homogeneously distributed around the calcium ion at an average distance of 2.374 Å. The fit also shows that 4.5 (±2) carbon atoms are present in the second co-ordination shell, of these 3 (±1) are located at a distance of 3.36 Å from calcium, and the others at 3.03 Å. These distances are longer than those in monohydrocalcite. This is not surprising, as shorter distances imply closer packing, which is characteristic of crystalline material.

The EDS measurements show that the antler spicules contain 14 mole% phosphate. The IR spectrum of these spicules, however, shows that a separate major phosphate phase does not exist. In the EXAFS analysis the addition of phosphate was examined in order to evaluate the possible contribution of its presence to the spectrum. The resulting fit did not, however, justify such a contribution.

Amorphous calcium carbonate from plant cystoliths (*Ficus retusa*) was studied using EXAFS by Taylor *et al.*[21] Interestingly, a comparison of their results to those for the antler spicules reveals significant differences in the calcium co-ordination shells. In the spicules 4.5 (±2) carbon atoms are found in the second shell, whereas only 1.5 carbon atoms were found in the second shell of the cystoliths.[21] It is worth stressing that the differences in the fit are not model dependent, as substantial differences are evident even in the Fourier transform of the original spectra. While there is hardly any structure (very low peaks) above the first shell in the Fourier-transformed cystoliths spectrum, a clear peak of a second shell exists in the Fourier-transformed spectrum of the antler spicules. TGA measurements of cystoliths from *Ficus microcarpa* (data not shown) show the same stoichiometry as do the antler spicules, namely one water molecule per carbonate ion. This leads to the conclusion that, although plant cystoliths and antler spicules are both regarded as being composed of amorphous calcium carbonate, their structures are different.

This in turn raises the broader possibility that similar detailed characterizations of the short-range structures in other biogenic amorphous calcium carbonate phases will also reveal significant differences. If so, these differences may well shed some light on their varied structure–function relations. Another intriguing possibility is that precursor amorphous calcium carbonate phases, such as that reported by Beniash *et al.*,[9] may already have the nascent short-range order that defines the transformation pathway into the mature phase.

Conclusion

The results reported here show that the short-range structure of the *Pyura pachydermatina* spicules is different from that reported for plant cystoliths. Thus the amorphous calcium carbonates should be considered as a group of different mineral phases. Characterization of their structures may provide information on their mechanisms of formation, transformation, stabilization, and eventually on their function.

Acknowledgements

We are grateful to Prof. G. Lambert for providing us with the spicules. We thank the beam line (X19A) scientists Dr Miller and Dr Kahlid. We also thank Dr Frenkel and Kleifeld for their advice and help in the EXAFS analysis and Dr Bouropoulos for his assistance with the X-ray measurements. S. W. is incumbent of the I. W. Abel Professorial Chair of Structural Biology, and L. A. is incumbent of the Dorothy and Patrick Gorman Professorial Chair. This work was supported by a United States–Israel Binational Foundation grant and by the Minerva foundation.

References

1 H. A. Lowenstam and S. Weiner, *On Biomineralization*, Oxford University Press, New York, 1989.
2 K. Simkiss, in *Biomineralization 93*, ed. D. Allemand, Musee Oceanographique, Monaco, 1993, pp. 49–54.

3 C. C. Perry in *Biomineralization, Chemical and Biochemical Perspectives*, eds. S. Mann, J. Webb and R. J. P. Williams, VCH, Weinheim, 1989, pp. 223–256.
4 Y. Zhou, K. Shimizu, J. N. Cha, G. D. Stucky and D. E. Morse, *Angew. Chem., Int. Ed.*, 1999, **38**, 780.
5 N. Kröger, R. Deutzmann and M. Sumper, *Science*, 1999, **286**, 1129.
6 G. H. Nancollas, in *Biomineralization*, *Chemical and Biochemical Perspectives*, eds. S. Mann, J. Webb and R. J. P. Williams, VCH, Weinheim, 1989, pp. 157–187.
7 H. A. Lowenstam and S. Weiner, *Science*, 1985, **227**, 51.
8 G. L. Decker and W. J. Lennarz, *Development*, 1988, **103**, 231.
9 E. Beniash, J. Aizenberg, L. Addadi and S. Weiner, *Proc. R. Soc. London*, *Ser. B*, 1997, **264**, 461.
10 L. Brecevic and A. E. Nielsen, *J. Cryst. Growth*, 1989, **98**, 504.
11 H. Setoguchi, M. Okazaki and S. Suga, in *Origin*, *evolution*, *and modern aspects of biomineralization in plants and animals*, ed. R. E. Crick, Plenum Press, New York, 1989, pp. 409–418.
12 A. P. Vinogradov, *The elementary chemical composition of marine organisms*, Sears foundation for marine research, New Haven, 1953.
13 J. Aizenberg, G. Lambert, L. Addadi and S. Weiner, *Adv. Mater.*, 1996, **8**, 223.
14 G. Lambert, C. C. Lambert and H. A. Lowenstam, in *Skeletal Biomineralization: Patterns*, *Processes and Evolutionary Trends*, ed. J. G. Carter, Van Nostrand Reinhold, New York, 1990, pp. 461–469.
15 H. A. Lowenstam, *Bull. Mar. Sci.*, 1989, **45**, 243.
16 G. Lambert and C. C. Lambert, *Connect. Tissue Res.*, 1996, **34**, 263.
17 G. L. Becker, C. H. Chen, J. W. Greenwalt and A. L. Lehninger, *J. Cell Biol.*, 1974, **61**, 316.
18 B. Dickens and W. E. Brown, *Inorg. Chem.*, 1970, **9**, 480.
19 J. R. Clarkson, T. J. Price and C. J. Adams, *J. Chem. Soc.*, *Faraday Trans.*, 1992, 243.
20 M. Prenant, *Bull. Biol.*, 1928, **62**, 21.
21 M. G. Taylor, K. Simkiss, G. N. Greaves, M. Okazaki and S. Mann, *Proc. R. Soc. London*, *Ser. B*, 1993, **252**, 75.
22 G. Lambert, *Acta Zool.*, 1992, **73**, 237.
23 E. Stern, M. Newville, B. Ravel, Y. Yacoby and D. Haskel, *Physica B*, 1995, **208/209**, 117.
24 Atoms.inp Archive. http://cars.uchicago.edu/~newville/adb/
25 R. W. G. Wyckoff, *Crystal Structures I*, Wiley and Sons, New York, 1963, p. 362.
26 H. Effenberger, *Monatsh. Chem.*, 1981, **112**, 899.
27 S. I. Zabinsky, J. J. Rehr, A. Ankudinov, R. C. Albers and M. J. Eller, *Phys. Rev. B*, 1995, **52**, 2995; J. J. Rehr, D. L. J. Mustre, S. I. Zabinsky and R. C. Albers, *J. Am. Chem. Soc.*, 1991, **113**, 5135; A. Ankudinov, Ph.D. Thesis, University of Washington, 1996.
28 I. Sagi and R. M. Chance, *J. Am. Chem. Soc.*, 1992, **114**, 8061; R. A. Scott, *Methods Enzymol.*, 1985, **117**, 414.
29 O. Kleifeld, A. Frenkel, O. Bogin, M. Eisenstein, V. Brumfeld, Y. Burstein and I. Sagi, *Biochemistry*, in the press.
30 H. Effenberger, K. Mereiter and J. Zemann, *Z. Kristallogr.*, 1981, **156**, 233.
31 M. I. Kay, R. A. Young and A. S. Posner, *Nature* (*London*), 1964, **204**, 1050.